Ab initio studies of hydrocarbon adsorption on stepped diamond surfaces

Dominic R. Alfonso
Department of Chemistry and Condensed Matter and Surface Sciences Program, Ohio University, Athens, Ohio 45701-2979

Sang H. Yang
Department of Physics, University of Illinois, Urbana, Illinois 61801

David A. Drabold
Department of Physics and Astronomy and Condensed Matter and Surface Sciences Program, Ohio University, Athens, Ohio 45701-2979

(Received 19 May 1994)

We present theoretical investigations of various hydrocarbon species adsorbed on hydrogenated flat (100), flat (111), and stepped (100) surfaces of diamond. We use *ab initio* density-functional molecular-dynamics simulations and a dynamical quenching minimization algorithm to calculate adsorption energies and minimum-energy configurations of different binding configurations. The onefold adsorption energies of the hydrocarbon fragments on all the surfaces were found to be in the order $E_{C_2H} > E_{CH_2} > E_{CH_3} > E_{C_2H_2}$. C_2H_2 is predicted to have stable twofold binding sites on both the terrace site and near step edges of the diamond (100) substrate. Adsorption on the flat (111) surface is found to be weaker compared to binding on the flat and stepped (100) substrates. We found several adsorption configurations where adsorption energies on the near step edges are different from those on the flat terrace. We studied local surface relaxations due to the adsorbed molecule. The binding of the hydrocarbon admolecule in the presence of an adsorbate is investigated. In general, we found weaker binding for molecules adsorbed on adjacent surface radical sites. Preliminary results on hydrocarbon adsorption at finite temperature are discussed.

I. INTRODUCTION

Considerable progress has been made in the area of low-temperature and low-pressure synthesis of diamond films.[1] This is motivated by the great technological importance of diamond and the success in forming thin diamond overlayers on other substrates besides diamond.[2–4] To realize the possibility of diamond films being used for commercial applications, it is necessary to gain a breakthrough in the controlled growth of these materials. To this end, particular attention has begun to focus on understanding the underlying growth mechanisms. Knowledge of the fundamental physical and chemical processes involved in the film growth will be helpful in identifying the factors that are at present limiting the quality of the films produced.

There have been numerous studies implicating hydrogen atoms and various hydrocarbon growth species as playing relevant roles during deposition.[5–12] H atoms are believed to be a generator of surface radical sites required for subsequent addition of growth species, and a destabilizer of the graphite phase, thus enhancing diamond growth. The identity of the growth species remains controversial. Several investigators have forwarded the methyl radical (CH_3) as the growth molecule.[13] On the other hand, Huang *et al.* and Frenklach and Spear suggested acetylene (C_2H_2) as the species responsible for diamond growth.[14,15] Martin and Hill proposed the idea that both CH_3 and C_2H_2 can be responsible for diamond formation.[10] Recently, Belton and Harris[16] and Frenklach[17] proposed mechanisms that assume growth via alternate addition of CH_3 and C_2H_2 molecules.

All of the investigations mentioned above have one essential feature—the incorporation of hydrocarbon species on the growing surface. The transport of these activated molecules and their subsequent adsorption to surface sites on the substrate is also probably important for diamond formation. It is, therefore, of utmost interest to study the adsorption of various hydrocarbon species on diamond surfaces. Investigation of hydrocarbon adsorption on diamond surfaces has received increasing attention.[18–25] Recently, Larrson *et al.* used an *ab initio* molecular orbital scheme to study the chemisorption of H and several hydrocarbon molecules on the (111) surface of diamond.[25] Using a density-functional method, Mintmire *et al.* and Pederson *et al.* calculated the binding energies of several one- and two-carbon species to the (111) diamond phase.[20,21] Frauenheim and Blaudeck studied several elementary reaction mechanisms for interaction of C_xH_y fragments with clean and with partly or fully hydrogenated diamond (111) surfaces using a semiempirical density functional approach.[22] Mehandru and Andersson used a semiempirical technique to look into the binding and migration of H, CH_2, CH_3, and C_2H_2 on both the (100) and (111) surfaces[18,23] while Brenner employed a semiempirical potential to study the adsorption of various hydrocarbons on the diamond (111) surface.[19]

 ©1994 The American Physical Society

Most of these studies, however, do not provide information regarding adsorption on stepped surfaces. In fact, diamond surfaces may contain stepped structures with height variations of hundreds of Å.[26] Zhu and co-workers suggested that growth may occur at the steps as revealed by their scanning-tunneling-microscopy and atomic-force-microscopy experiments.[27,28] Employing reflection-electron microscopy Hu *et al.* suggested that epitaxial growth may involve lateral motion of the steps, which is faster than the vertical growth rate.[29] The first attempt in the direction of obtaining knowledge about binding on step structures was based on the modified neglect of differential overlap (MNDO) studies undertaken by Zhu *et al.*[27] Recently, we performed adsorption studies of several hydrocarbon species on diamond flat and stepped (100) stepped surfaces using a semiempirical potential.[30] Our results showed small variations in the binding energies of hydrocarbons adsorbed on either flat terraces or near step edges. This surprising result motivated us to do a set of higher level calculations to explore hydrocarbon adsorption near step edges of diamond surfaces. To our knowledge, this is the first attempt to make a systematic comparison between hydrocarbon binding on the flat and on the stepped structures of diamond using the first-principles method.

In this paper, we perform first-principles studies to simulate interactions of CH_3, CH_2, C_2H, and C_2H_2 species with the near terrace site of diamond (100) and (111) surfaces and with the near step edges of the (100) diamond substrate. The (100) and (111) surfaces of diamond are commonly used as starting materials for homoepitaxial diamond film growth in a chemical vapor deposition (CVD) environment. The admolecules considered in this work are found to be present in the gas phase during film growth.[31] We address several issues: (1) single hydrocarbon adsorption on the flat (100) and (111) terrace vs near stepped edges of the (100) surface of diamond and (2) the effect of the presence of a chemisorbed hydrocarbon on the binding of an admolecule. We used *ab initio* molecular-dynamics (MD) simulations and dynamical quenching minimization techniques to obtain the adsorption energies and minimum-energy configurations of the admolecule-substrate systems. (3) We also performed preliminary calculations to determine the effect of surface thermal disorder on the adsorption energy of an admolecule. Such calculations are a relevant initial step to understanding the role of temperature on the diamond growth processes.

Our results show that the trends in the onefold adsorption energies on all the types of diamond surfaces considered in this investigation are identical: $E_{C_2H} > E_{CH_2} > E_{CH_3} > E_{C_2H_2}$. Several twofold binding modes were studied for C_2H_2 on both the flat and stepped surfaces of the (100) phase, and single molecule adsorption on the trough site (along the [1 1 0] direction) on the (100) substrate is the most stable. We found adsorbate-induced local surface relaxations such as dimer buckling on the (100) substrate and surface carbon vertical displacement on the (111) surface. There are several cases where hydrocarbon adsorption is either preferred or unfavorable on the near step (100) edges with respect to binding on the flat (100) surface. Adsorption of CH_3 and C_2H on the S_A structure and of CH_2 on the $S_B(b)$ substrate are stronger while trough site binding of C_2H_2 on the S_B step surfaces are weaker. The variations in the energetics could either be attributed to factors such as steric interferences or surface lattice distortions. We found that two molecule adsorption on adjacent sites of the diamond surface tend to be weaker compared to single molecule adsorption.

A critical aspect of experimental work on diamond growth is the role of substrate temperature T_s during growth. It is well known that CVD grown diamond requires that the substrate be maintained at a temperature in the range 1000–1400 K.[32] Thus, this and all other zero-temperature calculations are not describing all the salient features of growth. It would seem that the missing ingredients are (1) increased surface reactivity induced by thermal disorder and/or (2) diffusion of growth species on the hot surface. A first step toward understanding (1) is offered in this work. In the present investigation, we estimate finite-temperature (1100 K) adsorption energies for a single CH_3 radical chemisorbed on various surface carbon radical sites on a clean diamond (100) surfaces. Our result indicates that the molecule is more bound to the surface at elevated temperature.

The methodology is discussed in Sec. II, while the results of the calculations are presented and discussed in Sec. III.

II. METHODOLOGY

We use first-principles molecular-dynamics simulations developed by Sankey and Niklewski in this work.[33] This method is founded upon density-functional theory (DFT) and its suitability for covalent systems such as C and Si is well proven and documented.[33–36] In particular, the method has been applied to the diamond (100) reconstruction and yielded results quite consistent compared to self-consistent plane wave calculations. The essential approximations are (1) a spin unpolarized non-self-consistent version of the DFT using the Harris functional, and the local density approximation (LDA);[37] (2) non-local, norm conserving pseudopotential of Bachelet-Hamman-Schlüter type;[38] (3) a minimal basis set where the local orbitals ($1s$ and $3p$ functions per site) have compact support, reflecting a confinement boundary condition (orbital confinement radii for C and H are 4.1 and 3.8 a.u., respectively).[33] The LDA exchange correlation term assumes the Ceperley-Alder form as parametrized by Perdew and Zunger.[39,40]

The diamond substrates were modeled as slabs with periodic boundary conditions in the two directions parallel to the surface (infinite in two dimensions). For the flat (100) and (111) surfaces, we utilized a slab consisting of 10 C layers with 8 C atoms per layer. Two special k points were employed to sample the Brillouin zone of the supercells.[41] The (100) face was exposed and reconstructed into a (2×1) dimerized surface terminated by H atoms while the exposed (111) face assumes a hydrogen covered bulk-terminated surface (see Fig. 1). The bottom

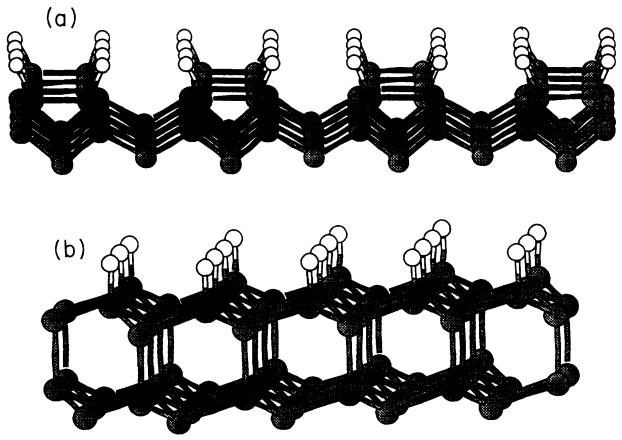

FIG. 1. Diagrams of (a) hydrogenated (100)-(2×1) and (b) hydrogenated (111) surfaces of diamond. Carbon atoms appear shaded.

layers of these slabs were passivated by H atoms. For the simulation system used in calculating energies near the step edges of the (100) surface, the S_A and S_B step types were created on a properly dimerized surface.[42] Employing Chadi's convention,[42] S_A represents a single atom step whose upper terrace contains dimers oriented perpendicular to the step edges, while S_B indicates a single layer step with dimers on the upper terrace oriented parallel to the step edge (see Fig. 2). Two types of S_B structures are considered in this work. One is the nonbonded type $S_B(n)$ with no rebonded atoms on the lower terrace, while the bonded type $S_B(b)$ had rebonded atoms present on the lower edge. The stepped structures models are five carbon layers deep where the bottom and the exposed upper layer are terminated by H atoms. Structures with S_A and S_B step edges have horizontal dimensions of 7×4 and 8×4 atoms per layer, respectively. The Γ point ($\mathbf{k} = \mathbf{0}$) was used to sample the small electronic Brillouin zone of the slab model for the stepped structures.

The minimum-energy configurations of our simulation systems were achieved using a dynamical quenching technique.[34] To reduce computational demands, the slab is first relaxed using semiclassical molecular-dynamics simulations based on Tersoff-Brenner semi-empirical potential expressions for the hydrocarbon system.[19] This potential, which has been used for diamond systems with great success, assumes the form

$$U = \sum_{j>i} [V_r(r_{ij}) - B_{ij} V_a(r_{ij})] , \tag{1}$$

where V_r and V_a are terms that represent pair-repulsive and pair-attractive interactions, respectively, while B_{ij} is a many-body bond-order term which depends on atomic coordination and angles.[19,43] This potential is based on a Tersoff bond-order expression which contains terms that correct for overbinding of radicals and consider nonlocal effects.[19] We then take this initially relaxed structure and further minimize it using an *ab initio* scheme until the forces experienced by each atom is less than 0.02 eV/Å. We performed a spot check wherein we relaxed a smaller diamond flat (100) slab model (4 C atom deep with 8 C atoms per layer) using combined semiclassical-*ab initio* scheme and comparing the structure with that obtained by employing *ab initio* methods alone. We found no significant variations between the resulting structures of the slabs. The adsorption energies that are cited below are defined as the total energy of the surface-adsorbate sys-

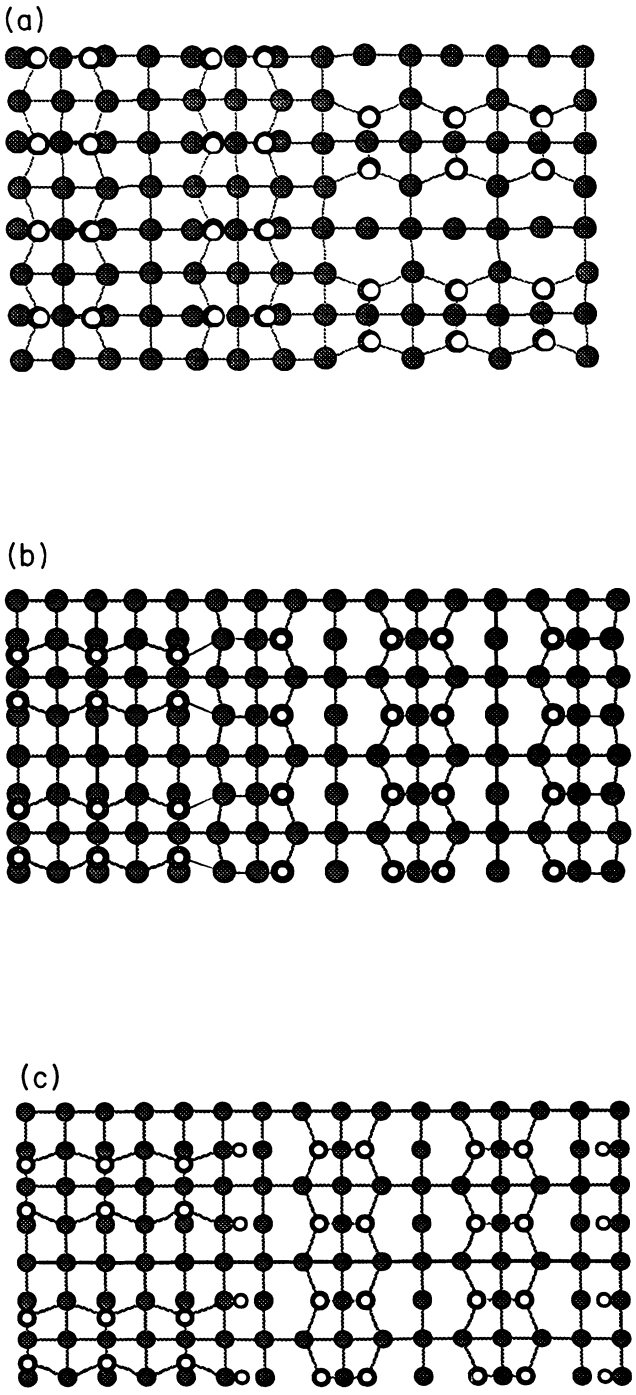

FIG. 2. The three types of diamond (100) stepped structures: (a) S_A, (b) $S_B(b)$, and (c) $S_B(n)$. Portions shown are the supercells for each step employed in this work (periodic 7×4 for the S_A structure and periodic 8×4 for the S_B structure). Carbon atoms appear shaded.

tem minus the total energy of the bare surface minus the energy of the isolated molecule. All relaxation effects of both the adsorbate and surface are included in our calculations.

In this work, we present structural and energetic information about growth. All experiences indicate that structural predictions by the present method are highly reliable. In fact, *without exception*, the present method gives nearly identical results with self-consistent plane wave methods for covalent systems as in the present problem. Moreover, energy *trends* are also to be considered as reliable for energy differences greater than $\approx$ 0.02 eV/atom. A quantitative statement about absolute energetics is a more delicate matter for our work and other studies in this area. Within our method there are three limitations in this connection, (1) the local density approximation (which tends to overbind), (2) the method assumes a spin unpolarized system, so effects connected with unpaired spins may not be well reproduced (in fact, this is usually a small effect in surface problems), and (3) because our local basis functions are confined[33] (which artificially increases the isolated atom kinetic energy), simple calculations of cohesive energy using the isolated atomic total energies as reference also tends to lead to overbinding. It is important to note that this in *no way* affects the quality of the electronic states or interatomic forces.

Other methods suffer from related limitations. Basis related limitations are well known in quantum chemistry methods [Møller-Plesset perturbation theory (MP2) method for example[25]], as are difficulties in treating the electron correlation energy with Hartree-Fock techniques. Also, these calculations are limited to very small systems because of the proliferation of matrix elements as the system size increases. However, it must be emphasized that these calculations have a different set of problems than our approach and the two approaches are helpful in understanding each others limitations.

Semiempirical methods can be devised to give specific energetics for geometries fit to. However, there is no guarantee that predictions are transferable to significantly different bonding environments. It is likely that these techniques will be most reliable near the structure fit to (typically a molecular and surface database), but will become increasingly unreliable in highly disordered environments. Of course, these methods have the great virtue that very large systems can be described in contrast to most electronic structure calculations.

III. RESULTS AND DISCUSSION

A. Hydrocarbon adsorption on flat (100) and (111) diamond surfaces

In this subsection, we discuss adsorption of single hydrocarbon molecules on the near terrace site of diamond (100) and (111) surfaces. The binding of these molecules was investigated in the presence of hydrogen vacancies on the surface. For onefold coordination of these fragments to the (100) surface, a hydrogen bonded to a surface dimer carbon is removed and replaced by the molecule. We also consider twofold coordination sites, which are relevant to the C_2H_2 molecule whose two carbons can simultaneously bond to surface radicals. These sites are (a) the bridge site, where the two-carbon molecule sits over two carbons belonging to the dimer pair and (b) trough sites, where C_2H_2 bridges surface carbons belonging to adjacent dimer pairs along either the [1 $\bar{1}$ 0] or [1 1 0] direction. The C–C bond of the molecule is placed parallel to the surface. To quantify the energetics of adsorption on the H terminated (111) surface, a onefold radical site is generated on the surface by removal of a hydrogen from the surface. An admolecule is placed on top of the dangling bond to simulate hydrocarbon adsorption on the (111) surface. All the sites described above are shown in Fig. 3. All the configurations were relaxed to their minimum energy state using an *ab initio* MD scheme and a dynamical quenching technique as described above. Table I lists the adsorption energies, intramolecular C–C bond lengths and the resulting distance of the bond formed by each molecule with the flat (100) and (111) diamond substrate after relaxation of the simulation systems. Figure 4 shows typical examples of the hydrocarbon bonded to the diamond surface.

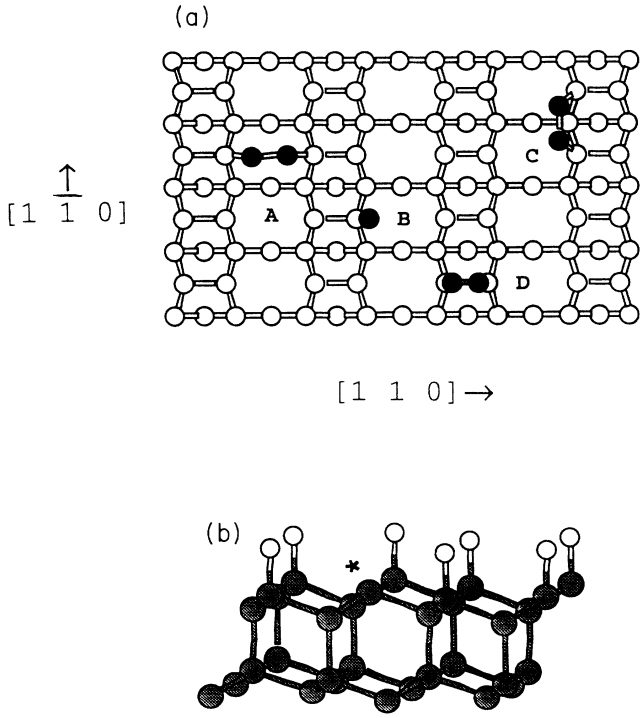

FIG. 3. (a) Top view of the diamond (100)-(2×1) surface showing various adsorption sites for the hydrocarbon adspecies. Shaded balls represent one- and two-carbon adspecies while white balls represent the substrate carbon atoms. *A* is a trough site along the [1 1 0] direction, *B* is a onefold binding site, *C* is a trough site in the [1 $\bar{1}$ 0] direction, and *D* is a bridge site. (b) Side view of a portion of a diamond (111) surface where the shaded balls represent the surface carbon. The marked atom is a radical surface carbon where the various hydrocarbon species are adsorbed.

TABLE I. Structural parameters for various single hydrocarbon molecule adsorbed on radical sites of hydrogenated (100)-(2×1) and (111) surfaces of diamond.

	E_b (eV)[a]	$r(C_s–C_a)$ (Å)[b]	$R(C_z–C_a)$ (Å)[c]
Diamond (100)			
CH_3	3.36	1.64	
C_2H	7.24	1.47	1.21
CH_2 (onefold)	4.68	1.54	
(bridge)	3.54	1.49/1.64[d]	
C_2H_2 (onefold)	0.52	1.59	1.33
(bridge)	2.89	1.54	1.35
(trough[1 1 0])	4.91	1.57	1.37
(trough[1 $\bar{1}$ 0])	4.17	1.55	1.36
Diamond(111)			
CH_3	2.68	1.74	
C_2H	7.05	1.46	1.19
CH_2	3.76	1.53	
C_2H_2	no binding		

[a] E_b refers to the adsorption energy.
[b] $r(C_s–C_a)$ refers to the length of the bond formed by the admolecule with the substrate.
[c] $r(C_a–C_a)$ denotes the intramolecular C–C distance for the two-carbon adsorbate.
[d] Bond lengths of CH_2 with the carbon dimers.

1. *Structure of the adsorbate-substrate systems*

Analysis of the minimum-energy configurations for the various admolecule-substrate systems show the occurrence of structural relaxations associated with chemisorption. The results of the simulations reveal that with the exception of C_2H chemisorbed on the (111) surface, there is a significant change in the internal structure of the molecule after binding to the surface. A free methyl radical CH_3, for example, is a planar species but assumes an umbrellalike structure tilted by about 14° from the surface normal after forming a bond with the (100) surface. Likewise, the same admolecule has an umbrella-type configuration when chemisorbed to the (111) surface. Not surprisingly, the C_2H molecule did not retain its linear geometry after coordinating with the (100) surface due to steric repulsion induced by the surface H. The acetylene molecule loses its linear structure after being incorporated to the surface. Moreover, inspection of Table I shows that the intramolecular C–C bond lengths for the bound C_2H_2 approach values which lie between the double and the triple C–C bond lengths. Such bond-order reduction was not observed for the C_2H adsorbed to the (100) and (111) substrates.

The calculations likewise predict local surface relaxations induced by adsorbates which are onefold coordinated to either (100) or (111) substrate. The surface carbon at which the molecule is bonded relaxed outwardly from its original bulk position. These atomic displacements were typically about 0.1 Å. For the (100) surface, this adsorbate-induced relaxation caused buckling of the surface dimer whose one member carbon is bonded to the admolecule. For trough site adsorption of C_2H_2, there is also a buckling of the adjacent dimers (along [1 1 0] or [1 $\bar{1}$ 0]) which the molecule bridges. On the other hand, no surface dimer buckling is found for bridge site adsorption of C_2H_2.

2. *Adsorption energies*

The ordering of the adsorption energies for all species can be obtained from Table I. For onefold adsorption to

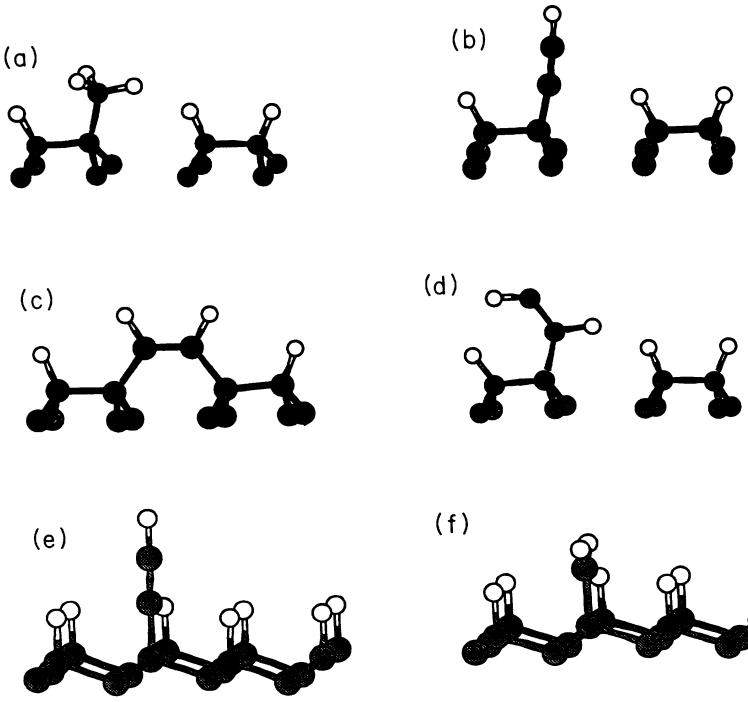

FIG. 4. Selected examples of configurations of the hydrocarbon admolecules on the flat diamond (100) and (111) surfaces. (a) CH_3 on (100), (b) C_2H on (100), (c) C_2H_2 on (100) (trough site along the [1 1 0] direction), (d) C_2H_2 on (100) (onefold), (e) C_2H on (111), and (f) CH_2 on (111).

the (100) surface, the energy trend was found to be: $E_{C_2H} > E_{CH_2} > E_{CH_3} > E_{C_2H_2}$. C_2H forms the strongest single bond without significant change in the C–C bond length of the molecule. Although the gas phase concentration of C_2H in a typical hot-filament CVD system is significantly lower compared to species such as the methyl radical and acetylene,[31] its large binding energy indicates that it might be an important growth species. The molecule CH_2 and CH_3 also form a strong single bond with the surface. Compared to the other admolecule considered in this work, C_2H is the most unstable and reactive species in the gas phase.[44] This molecule, therefore, forms the strongest bond with the surface radical. CH_2 binds more strongly than CH_3 because of less steric hindrance from the additional H on the methyl radical. We found a less stable twofold binding mode for CH_2 where it bridges carbons belonging to the dimer pair. Unlike the onefold CH_2 bonding where the molecule forms a single bond with the surface radical, the two-fold binding configuration is characterized by formation of a bond with each surface carbon belonging to the dimer pair. This configuration, however, is found to be more strained due to enhanced steric repulsion between the admolecule and the surface H that is bonded to the dimer bridged by the admolecule. This less preferred binding mode for CH_2 was also predicted from theoretical work based on MNDO calculations.[45] Recent semiclassical MD simulations indicate that the onefold addition of CH_2 and CH_3 on the radical site of the hydrogenated(100)-(2×1) diamond surface at around 1200 K is responsible for the initial growth of the film.[24] Our simulations predict that the adsorption of these molecules to a radical site on the (100) surface is energetically favorable.

A weak onefold binding mode of the admolecule C_2H_2 on the diamond (100) surface is predicted (adsorption energy=0.52 eV). The structural constraint of the lattice and the steric repulsion due to surface hydrogens caused the adsorbed molecule to assume a distorted geometry where the intramolecular C–C bond points to the vacuum. This finding seems to indicate that onefold adsorption of C_2H_2 is not a probable initial growth pathway. It is reasonable to expect that C_2H_2 can form a single bond with the surface, but the bond is weak enough that the molecule may desorb relatively quick. On the other hand, we found a more stable binding configuration where the molecule is twofold coordinated with the surface. Of these three twofold-type interaction sites, the one with the C_2H_2 bridging two adjacent dimers along the [1 1 0] direction is predicted to be the most stable. These more stable binding configurations can be a plausible initial diamond growth pathway based on C_2H_2 as a growth species since it can lead to decomposition of the adsorbate which is a possibility at hyperthermal deposition conditions. These hypothetical mechanisms involving the chemisorption of acetylene and its subsequent decomposition were explored by Zhu and White.[46] Molecular-dynamics simulations of hyperthermal deposition of several acetylene molecules in the presence of gaseous H atom environment on a diamond (100) substrate is currently in progress and results will be presented in future publications.

The ordering of the adsorption energies of the molecules in the case where they are singly coordinated to the diamond (111) surface is identical to that found in the (100) surface. The molecule C_2H is found to be the most reactive species forming a strong single bond with a radical site on the (111) substrate. Similarly, CH_2 is more bound to the (111) surface than the methyl radical because of reduced steric interference on CH_2 due to the surface hydrogens. The adsorbed molecules CH_2 and CH_3 can be a possible site for subsequent reaction with gas phase hydrocarbons. The adsorbate CH_2 has a dangling bond which can react with gaseous hydrocarbon species while an additional carbon can be incorporated on the adsorbed methyl radical by abstraction of one of its hydrogens. Onefold binding of C_2H_2 to the (111) surface is predicted to be unstable. This result reveals that adsorption of C_2H_2 on a radical site on the (111) diamond surface through one of its carbons is probably not a reasonable preliminary growth pathway. Inspection of Table I shows that the one-fold hydrocarbon adsorption on the the (100) surface is generally more favored than on the (111) surface. These findings indicate that if *energetics are considered alone*, growth mechanisms seem to favor chemical reaction occurring on the (100)-(2×1) diamond surface.

3. Comparisons with previous work on hydrocarbon adsorption on the flat diamond (100) surface

Table II lists adsorption energies of hydrocarbon molecules on the diamond (100) surface obtained from previous theoretical investigations. The adsorption of hydrocarbon molecules such as CH_3, CH_2, and C_2H_2 on the hydrogenated diamond (100)-(2×1) surface was investigated by Mehandru and Andersson employing atom-superposition and electron delocalization molecular orbital methods (ASED-MO).[23] The adsorption energies for onefold coordination with the surface were estimated to be in the following order: $E_{CH_2} > E_{CH_3} > E_{C_2H_2}$ (no binding). The onefold adsorption energies that they calculated for CH_2 and CH_3 are 4.38 eV and 3.38 eV, respectively. They found a more stable twofold binding configuration for CH_2 (adsorption energy=6.30 eV) where the molecule bridges a dimer pair. Of the twofold binding modes for C_2H_2 that they considered, the one where the molecule bridges two adjacent dimers (trough site) along the [1 1 0] direction is the more preferable. The computed C_2H_2 trough site and bridge site energies are 3.80 eV, and 3.20 eV, respectively. Alfonso *et al.* recently performed semiclassical MD simulations to calculate adsorption energies of various hydrocarbons on the diamond (100) surface.[30] The predicted ordering of the binding energies is: $E_{CH_2} > E_{C_2H} > E_{CH_3} > E_{C_2H_2}$, $E_{C_2H_4}$ (no binding). The calculation yields essentially similar energy for onefold and bridge site binding for CH_2 (4.59 eV vs 4.67 eV). Similarly, a C_2H_2 bridging adjacent dimers along the [1 1 0] directions was predicted to be the more stable conformation for twofold binding of the molecule. The binding energies for the molecule trough

TABLE II. Energies (eV) for a single C_xH_y fragment adsorbed on the hydrogenated (100)-(2×1) surface of diamond. All entries that are not labeled refer to onefold adsorption energies.

Reference	C_2H	CH_2	CH_3	C_2H_2	Method
23		4.38	3.38	no binding	ASED-MO
		6.30 (bridge)		3.20 (bridge)	
				3.80 (trough[1 1 0])	
26	4.34	4.59	4.18	no binding	empirical potential
		4.67 (bridge)		3.62 (bridge)	
				6.54 (trough[1 1 0])	
Present study[a]	7.24	4.68	3.36	0.52	*ab initio* MD
		3.54 (bridge)		2.89 (bridge)	
				4.91 (trough[1 1 0])	

[a]Results from Table I.

site and bridge site adsorption are 6.54 eV and 3.62 eV, respectively.

The present work agrees with the calculations cited above in the trend in binding energies for onefold adsorption of C_2H, CH_3, and C_2H_2 and for the twofold binding of C_2H_2. We, however, found that the bridge site adsorption is the less preferred configuration for CH_2. Unlike the semiclassical calculations, the molecule C_2H is more bound to the surface than CH_2, which, as mentioned previously, is due to the fact that the C_2H molecule is the least stable species. Moreover, we find the small binding energy for C_2H_2 singly coordinated to the surface. A quantitative comparison of the adsorption energies (see Table II) shows that with few exceptions, there is some discrepancy between the present results for energies of C_2H, CH_2 (onefold/bridge), CH_3 and C_2H_2 (onefold/bridge/trough[1 1 0]) and the semiclassical MD results reported by Alfonso *et al.*,[30] or the ASED-MO values for CH_2 (onefold/bridge), CH_3 and C_2H_2 (onefold/bridge/trough[110]) reported by Mehandru and Andersson.[23]

4. Comparisons with previous work on hydrocarbon adsorption on the flat diamond (111) surface

Table III summarizes the results from previous theoretical works on single hydrocarbon binding on the (111) surface of diamond. Employing the ASED-MO scheme, Mehandru and Andersson studied hydrocarbon binding with the hydrogenated (111) surface of diamond and the adsorption energies were found to have the order: $E_{C_2H} > E_{CH} \approx E_{CH_2} > E_{CH_3} > E_{C_2H_2}$ (no binding).[18] The adsorption energies for C_2H, CH_2, CH_3, and CH that they reported are 5.39, 3.99, 3.07, and 4.12 eV, respectively. Using an empirical potential expression, hydrocarbon energetics on the (111) surface were found to be in the following order: $E_{C_2H} > E_{CH_3} > E_{C_2H_2}$ (no binding).[18,47] Mintmire *et al.* and Pederson *et al.* used the local density approximations scheme and the adsorption energies obtained for C_2H, CH_3, and C_2H_2 were estimated to be in the order: $E_{C_2H} > E_{CH_3} > E_{C_2H_2}$.[20,21] Larsson *et al.* used the first-principles molecular orbital theory to investigate chemisorption of H and various hydrocarbons on the diamond (111) surfaces and the predicted ordering of hydrocarbon binding energies is $E_{C_2H} > E_{CH_2}$ (singlet) $> E_{CH} > E_{CH_2}$ (triplet) $> E_{CH_3} > E_{C_2H_2}$.[25]

The trend in binding energies of C_2H, CH_2, CH_3, and C_2H_2 on the flat (111) surface found in the present work is in agreement with the semiempirical and the various first-principles investigations highlighted above. Quantitative comparisons (see Table III) show that the adsorption energies for C_2H, CH_2, CH_3, and C_2H_2 obtained in the present work is closer to the values obtained by Larrson *et al.* using second-order Møller-Plesset perturbation theory (MP2) scheme taking into account the basis superposition effects.[25] We, however, found less agreement upon comparing our numerical results for the adsorption energies of C_2H, CH_3, and C_2H_2 with the LDA

TABLE III. Onefold adsorption energies (eV) for a single C_xH_y fragment on the hydrogenated (111) surface of diamond.

Reference	C_2H	CH_2	CH_3	C_2H_2	Method
18	5.39	3.99	3.07	no binding	ASED-MO
19	3.9		3.7	no binding[b]	empirical potential
20	6.00		4.30	1.70	LDA
21	6.60		4.50	1.70	LDA
25	6.07	4.67	3.58	0.27	MP2
Present study[a]	7.05	3.76	2.68	no binding	*ab initio* MD

[a]Results from Table I.

[b]We did not find onefold binding for C_2H_2 using the empirical potential method.

results reported by Pederson *et al.*[21] and by Mintmire *et al.*[20] Moreover, the various first-principles studies cited yielded weak onefold coordination of C_2H_2 on the (111) surface while the present investigation did not give any stable structure for a similar configuration.

B. Hydrocarbon adsorption on stepped (100) diamond surfaces

In this subsection, hydrocarbon adsorption on the stepped (100) surfaces of diamond is investigated in the presence of carbon radical sites near step edges. For a onefold binding mode, a near step edge surface hydrogen is removed and replaced by the admolecule. In the case of twofold adsorption, a trough site and bridge site are created by the method described in subsection III A. Figure 5 shows typical binding sites for three types of stepped surface considered in this work. All the resulting slabs were relaxed to their minimum-energy structure employing *ab initio* molecular-dynamics simulations and the dynamical quenching method. Listed in Table IV are the adsorption energies of various adsorbed hydrocarbons while Fig. 5 shows typical minimum-energy configurations for the admolecule-stepped surface system.

1. Structure of the adsorbate-substrate systems

Similar to adspecies binding on the flat diamond surfaces, structural relaxations due to chemisorption were observed for hydrocarbon binding to the stepped (100) surfaces. Analysis of the structural parameters of the relaxed admolecule-substrate systems indicates a change in the internal configurations of all admolecules with respect to its gas phase structure and the relaxation of surface atoms as a result of chemisorption. The calculated bond lengths between the admolecule and stepped (100) substrate are comparable to those on the flat (100) surface. The average bond lengths between the C_2H and CH_2 molecules and the substrates are close to the bond length of graphite (1.42 Å) and diamond, respectively (1.52 Å).

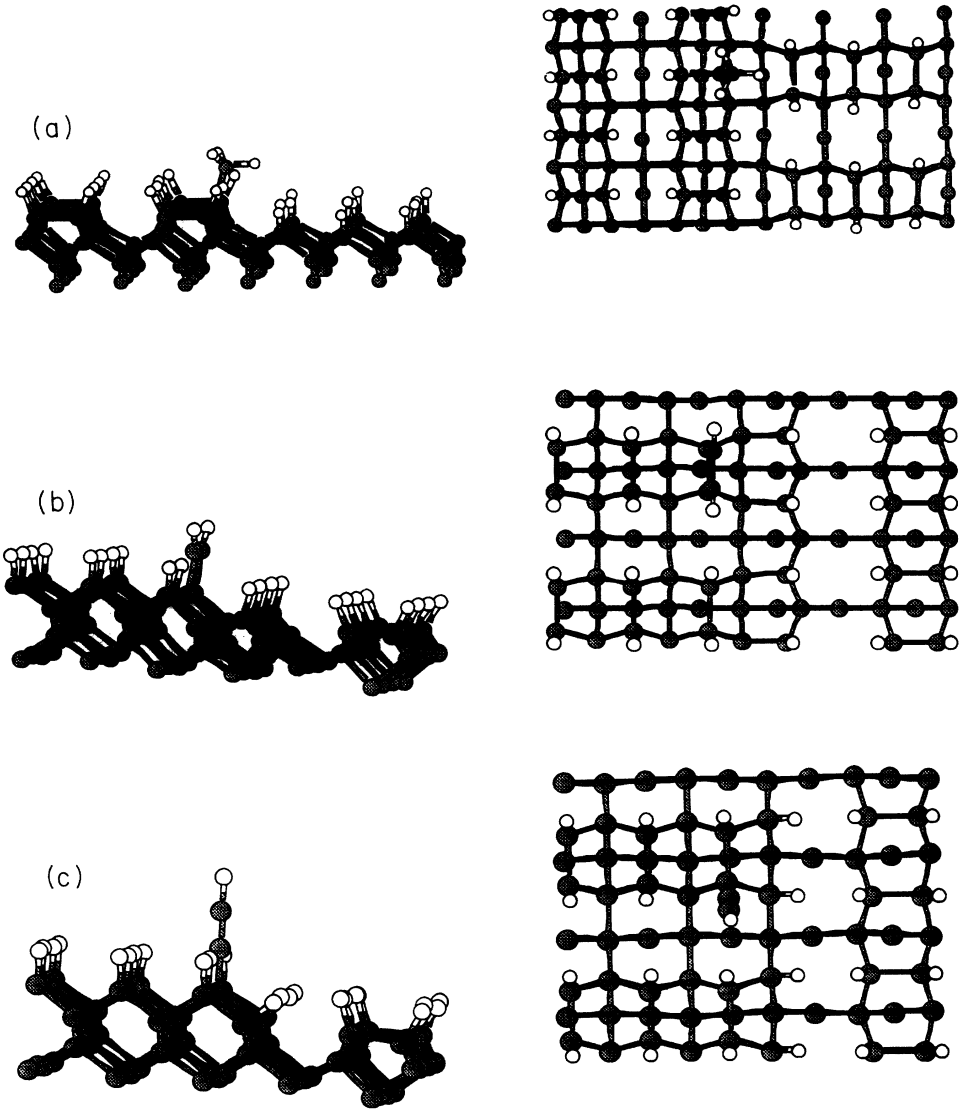

FIG. 5. Typical minimum-energy configurations for admolecule-stepped surface systems. Clusters shown are a portion of the unit cell employed in this work. (a) CH_3 on S_A, (b) C_2H_2 on $S_B(b)$ (bridge site), and (c) C_2H on $S_B(n)$. Carbon atoms appear shaded.

TABLE IV. Structural parameters for various single hydrocarbon molecules adsorbed on radical sites of different types of hydrogenated stepped (100) surfaces of diamond.

	E_b (eV)[a]	$r(C_2–C_a)$ (Å)[b]	$r(C_a–C_a)$ (Å)[c]
S_A			
CH_3	3.76	1.63	
C_2H	7.47	1.45	1.21
CH_2	4.44	1.50	
C_2H_2 (onefold)	0.39	1.62	1.29
(bridge)	2.87	1.53	1.36
$S_B(b)$			
CH_3	3.46	1.63	
C_2H	7.20	1.45	1.21
CH_2	5.09	1.52	
C_2H_2 (onefold)	0.71	1.57	1.33
(bridge)	2.88	1.54	1.35
(trough[1 1 0])	4.22	1.57	1.37
$S_B(n)$			
CH_3	3.48	1.63	
C_2H	7.30	1.45	1.20
CH_2	4.41	1.50	–
C_2H_2 (onefold)	no binding		
(bridge)	2.77	1.54	1.35
(trough[1 1 0])	3.95	1.57	1.37

[a] E_b refers to the adsorption energy.

[b] $r(C_s–C_a)$ refers to the length of the bond formed by the admolecule with the substrate.

[c] $r(C_a–C_a)$ denotes the intramolecular C–C bond length for the two-carbon adsorbate.

The CH_3 radical binds singly to the surface with the bond length longer than those found in diamond. The intramolecular bond distances for the adsorbed two-carbon species are also similar to those adsorbed on the flat (100) substrate. There is a drop in the C–C bond length in the acetylene molecule due to its interaction with the substrate. The C_2H molecule chemisorbed to the surface, with its C–C bond length practically unchanged.

Except for C_2H, onefold coordination of the molecules with the stepped structure produces dimer buckling whose one member carbon is bonded to the adspecies. The buckling originates from an average vertical displacement from its bulk position (about 0.06 Å) of the surface carbon where the admolecule is coordinated. Similarly, we predict buckling of adjacent surface dimers due to trough site adsorption of C_2H_2. Inspection of the configurations of C_2H_2 adsorbed on the S_B step structures shows that the admolecule induces inward displacements (about 0.08 Å) of the surface carbons where it is coordinated. Sinking of these surface carbons to the substrate network causes buckling of adjacent dimers whose carbons are coordinated to the admolecule. On the other hand, bridge site coordination of C_2H_2 did not induce buckling to the dimer where it is coordinated but we found reduction of the bond length of the said surface dimer by about 0.05 Å.

2. *Adsorption energies*

The ordering of the adsorption energies for onefold binding on all stepped structures is identical to the trend found for the flat (100) surfaces. The adsorbate C_2H binds strongly to the step edges while onefold coordination of the acetylene molecule with the S_A and $S_B(b)$ step edges are weak (no stable onefold interaction between acetylene and $S_B(n)$ is found). To determine which binding configuration is more stable for CH_2, we did a spot check by calculating the energy for CH_2 which bridges a carbon dimer (twofold bonding configuration) near the step edges of the S_A structure. We found that similar to CH_2 binding on the flat (100) surface, the bridgelike configuration is less stable than the corresponding one-fold interaction. Table IV shows that CH_2 forms a stronger single bond to the step structures compared to the methyl radical.

Comparison of admolecule binding energies shows that binding on the stepped (100) substrate is preferred over binding on the flat (111) surface. The increase in binding can be attributed to the lesser steric interference experienced by the admolecule adsorbed on the near step edges of the (100) diamond surface. Comparison of the hydrocarbon binding energies on the stepped structures and on the flat (100) surface allow interesting conclusions. (1) C_2H and CH_3 are found to bind more strongly to step edges of the S_A substrate while its energies on both $S_B(n)$ and $S_B(b)$ steps show little variation with respect to its energies on the flat (100) surface. Notice that there is a repulsive interaction between one of the methyl hydrogens or the carbons of C_2H and the surface H bonded on the nearest dimer along the [1 1 0] direction. Such repulsion is absent only when either molecule is adsorbed on the step edge of the S_A surface, making them more bound compared to the case where they are adsorbed on flat (100) or S_B structures. (2) For the admolecule CH_2, the most stable structure is predicted on the onefold site of the $S_B(b)$ step edges. The CH_2 molecule does not have a hydrogen that is oriented similar to one of methyl hydrogens but its hydrogens are subject to repulsive interaction to the adjacent surface hydrogens bonded on the nearest dimers along the [1 $\bar{1}$ 0] direction. Such a steric effect is minimized when the molecule is adsorbed on the S_B substrate, particularly on the S_B bonded-type structure. Such reasoning might lead us to conclude that the energy of CH_2 on the S_B nonbonded type should be favored over the flat (100) surfaces but the lower binding energy proves otherwise. Analysis of the stable structure of this molecule on the $S_B(n)$ surface yields a strained configuration which is probably due to the strain imposed by the lattice. The molecule is tilted by about 17° from the surface normal which is 5° bigger than its tilt on the flat (100) substrate. We also observed elongation of the dimer bond whose one member carbon is bonded to CH_2 by about 0.06 Å. These increases in the dimer bond and in the molecule tilt with respect to the surface normal and the drop in the adsorption energy were also predicted for CH_2 chemisorbed on the S_A stepped surface. (3) Twofold binding of acetylene is favored over single coordination, where the trough site adsorption is the most preferred

binding configuration. Binding on the near step edges trough site of the S_B surface is predicted to be less stable compared to a similar site on the flat (100) diamond surface. As mentioned above, trough site coordination of this molecule causes adjacent dimers to buckle. Inward displacements of these surface carbons yield a great deal of lattice distortion on the subsurface layer around both $S_B(n)$ and $S_B(b)$ step structures, which probably causes trough site binding on these steps which is less stable with respect to those on the flat (100) surface.

3. Comparisons with previous work

Recently, we performed a calculation using an empirical-potential expression to investigate the interactions of hydrocarbons with the stepped (100) surfaces.[30] The trend in the onefold binding energies of the admolecules obtained is identical to the present work. Similarly, both calculations reveal that trough site binding is the most energetically favorable for the molecule C_2H_2. However, our previous investigations show little variation in terms of the binding energies of hydrocarbons adsorbed on the flat (100) and on the stepped (100) surfaces.[30] Our *ab initio* results reveal several instances where hydrocarbon adsorption on the stepped (100) structure can be either preferable or unfavorable with respect to binding on the flat (100) surface.

C. Two-molecule adsorption

In this subsection, we investigate two hydrocarbon molecules adsorbed on selected adjacent surface carbon atoms on the diamond flat and stepped (100) surfaces. Such a coverage can be a possibility during epitaxial diamond growth. Our objective is to consider interaction between hydrocarbon fragments, and its effect on the equilibrium structure and adsorption energies of the coadsorbed molecules. We limited our investigation to the species CH_3 and C_2H_2 which are postulated as growth precursors. For coadsorption of a methyl radical on the flat substrate, we consider two bonding configurations (a) two CH_3 molecules adsorbed on carbons belonging to a dimer pair and (b) two molecules adsorbed on carbons belonging to an adjacent dimer pair along the [1 $\bar{1}$ 0] direction. The first site (onefold$_x$) is created by removing H atoms from a dimer pair and replacing each atom by the molecule while the second one (onefold$_y$) originates from the removal of H atoms from carbons belonging to the adjacent dimer pair in the [1 $\bar{1}$ 0] direction and replacing each by CH_3. For the methyl radical adsorption on the stepped (100) substrate, the appropriate onefold binding site is generated by the scheme discussed previously. Two possible binding configurations were considered for the acetylene coadsorption case, (a) two molecules adsorbed on adjacent bridge sites and (b) adjacent trough sites. The adjacent bridge and trough sites are created by the scheme discussed in subsection III A. The adjacent trough sites that we consider are the ones present along the [1 1 0] direction. All the simulation systems were relaxed using an *ab initio* scheme as discussed in Sec. II.

The predicted adsorption energy per molecule is shown in Table V. The most striking point that emerges is that there is a decrease in adsorption energies of the two adsorbed CH_3 molecules on the flat and stepped substrates compared to single molecule adsorption. These calculations show that the formation of such a structure is energetically prohibited with respect to single methyl radical adsorption. The unfavorable energetics can mostly be attributed to steric repulsion between the adsorbate hydrogens. For the configuration where each molecule is bonded to each carbon belonging to a dimer pair, we find that the two CH_3 groups experience symmetric tilting away from the surface normal. The tilt of each admolecule from the surface normal is about 20°, which is 6° larger with respect to single CH_3 adsorption geometry. In the other configuration where the radicals are adsorbed to the onefold$_x$ site, the adsorbed methyl radical is rotated by approximately 60° with respect to the other adsorbed molecule.

We next discuss coadsorption of acetylene on selected adjacent sites on the flat and stepped (100) surfaces. The calculated structure of each adsorbed molecule is essentially similar with respect to the single C_2H_2 geometry. This finding is different from the CH_3 coadsorption case, where a dramatic structural change occurs for both admolecules due to enhanced steric repulsion. For adsorption on adjacent bridge sites, we found no significant variation in the binding energies of the molecules. This indicates that such a structure is not energetically unfavorable compared to the single C_2H_2 adsorption case. However, there is a decrease in the binding energy for two-acetylene-molecule adsorption on the trough site of the flat (100) substrate. Each admolecule causes inward displacements of the surface carbon atoms that it bridges, resulting in the buckling of adjacent surface dimers. Such dimer buckling introduced great lattice distortions around the trough sites region resulting to less energetically favorable structures.

TABLE V. Adsorption energies (in eV/molecule) for two molecules adsorbed on selected adjacent radical sites of the flat (100) and different types of stepped (100) surfaces.

Molecule	Flat (100)	S_A	$S_B(n)$	$S_B(b)$
CH_3	2.80 (onefold$_x$) 2.07 (onefold$_y$)	2.90 (onefold$_y$)	3.00 (onefold$_x$)	2.88 (onefold$_x$)
C_2H_2	2.87 (bridge) 4.30 (trough[1 1 0])	2.65 (bridge)	2.89 (bridge)	2.79 (bridge)

D. Finite-temperature effect on the adsorption energy of methyl radical on nonhydrogenated flat (100) diamond surface

In this subsection, we present preliminary results concerning the effect of surface thermal disorder on the binding of hydrocarbon species. To this end, we compare CH_3 radical adsorption energies on the clean (100)-(2×1) diamond surface at two different temperatures T_s (T_s= 0 K and T_s= 1100 K.) The substrate is modeled using supercells of atoms periodic in two dimensions. The slab is 10 C atom layer thick containing 8 C atoms per layer. The bottom layer of the slab is terminated by hydrogens. The binding sites that we considered in this work are sites B [see Fig. 3(a), B_x, and B_y. Sites B_x and B_y are surface carbon atoms adjacent to site B along the [1 1 0] and the [1 $\bar{1}$ 0] directions, respectively.

To simulate CH_3 radical interaction with the clean substrate at a temperature equal to 0 K, we first relaxed the slab to its minimum-energy configuration using the *ab initio* scheme. We then put the admolecule on a surface binding site and the adsorption energy is crudely estimated by allowing only the admolecule to relax. For the higher-temperature case, the substrate is initially immersed in a 1100-K Berendsen thermostat[48] for about 1 ps. We then calculate the adsorption energy of a CH_3 species on a given surface site by allowing only the admolecule to relax in the presence of the frozen thermally disordered surface. We used two special k points to sample the Brillouin zone of our slabs.

The results of the simulations showed that the molecule is more bound (has higher adsorption energy) to sites B, B_x, and B_y of the higher-temperature thermally disordered substrate by about 1.04, 0.50, and 0.54 eV, respectively, compared to the T_s= 0 K surface. Although this spot calculation will *not* provide us a complete picture of diamond growth mechanisms at finite temperature, the striking results certainly implicate thermal disorder as one of the factors that might influence hydrocarbon binding to the surface. We are currently exploring the role of substrate temperature on admolecule adsorption and we intend to report comprehensive findings in a future paper. Moreover, as a first step in relating these and other findings to the electronic structures, we recently report band structure calculations of the clean and hydrogenated (100) surfaces of diamond.[35] No surface states are found for the H terminated surface, while we identified surface states associated with the clean surface. We intend to make a systematic study connecting electronic properties and the present results in a future publication.

IV. CONCLUSIONS

(1) We performed theoretical studies of adsorption of various hydrocarbon species such as CH_3, C_2H_2, CH_2, and C_2H on the flat (100), flat (111), and stepped (100) surfaces of diamond using first-principles molecular-dynamics simulations and a dynamical quenching minimization technique.

(2) The predicted energies for onefold binding of the admolecules to the various types of diamond surfaces are in the order: $E_{C_2H} > E_{CH_2} > E_{CH_3} > E_{C_2H_2}$. Several stable twofold binding modes were found for C_2H_2 and the configuration where the molecule bridges two adjacent carbon dimers along the [1 1 0] direction is the most energetically preferable.

(3) Hydrocarbon adsorption on the flat and stepped (100) diamond substrates are more favorable than on the flat (111) surface. There were adsorption configurations where admolecules binding on the stepped (100) structure is either preferred or less favorable with respect to bonding on the flat (100) substrate. These variations could originate from steric factors and strain imposed by the surface lattice.

(4) Coadsorption of the hydrocarbon molecules on adjacent sites of the flat and stepped (100) diamond surfaces is, in general, unstable with respect to single molecule adsorption.

(5) Preliminary results on finite-temperature adsorption studies of CH_3 bound to different radical sites on the unhydrogenated diamond (100) substrate indicate an increase in the adsorption energy of the molecule at 1100 K.

(6) Coordinates discussed in this paper are available upon request.[49]

ACKNOWLEDGMENTS

We are very grateful to S.E. Ulloa for his numerous valuable contributions to this present work. We thank D.W. Brenner for providing us the spline subroutines that we needed in our semiclassical MD code and for helpful discussions. We also thank M. Kordesch, D. Ingram, H. Richardson, and J. Adams for fruitful discussions. We acknowledge partial support from the Ohio Supercomputer Center through Project No. PHS060 and also from NSF Grant No. DMR-93-22412. We are grateful to the Minnesota Supercomputer Center for the XMOL graphics package which was used for all the figures in this paper.

[1] For reviews of diamond synthesis under metastable conditions see, R.C. DeVries, Annu. Rev. Mater. Sci. **17**, 161 (1987); J.C. Angus and C.C. Hayman, Science **241**, 913 (1988); K.E. Spear, J. Am. Ceram. Soc. **72**, 171 (1989).

[2] *Diamond and Diamond-Like Films and Coatings*, edited by R.E. Clausing, L.L. Hostou, J.C. Angus, and P. Koidl (Plenum, New York, 1991).

[3] C.V. Deshpandey and R.F. Bunshah, J. Vac. Sci. Technol. A **7**, 2294 (1989).

[4] F. Jansen, M.A. Machonkin, and D.E. Kuhman, J. Vac. Sci. Technol. A **8**, 3785 (1990).

[5] S.S. Lee, D.W. Minsek, D.J. Vestyck, and P. Chen, Science **263**, 1596 (1994).

[6] S.J. Harris and L.R. Martin, J. Mater. Res. **5**, 2313 (1990).

[7] W. Piekarczyk and W.A. Yarbrough, J. Cryst. Growth **108**, 583 (1991).

[8]S.J. Harris, Appl. Phys. Lett. **56**, 2998 (1990).
[9]C.J. Chu, M.P. D'Evelyn, R.H. Hauge, and J.L. Margrave, J. Mater. Res. **5**, 2405 (1990).
[10]L.R. Martin and M.W. Hill, J. Mater. Sci. Lett. **9**, 621 (1990).
[11]M. Frenklach and H. Wang, Phys. Rev. B **43**, 1520 (1991).
[12]F. Jansen, M.A. Machonkin, and D.E. Kuhman, J. Vac. Sci. Technol. A **8**, 3785 (1990).
[13]R. Mania, L. Stobierski, and R. Pampuch, Cryst. Res. Tech. **16**, 785 (1981); F.G. Celii, P.E. Pehrsson, H.T. Wang, and J.E. Butler, Appl. Phys. Lett. **52**, 2043 (1988).
[14]D. Huang, M. Frenklach, and M. Maroncelli, J. Phys. Chem. **92**, 6379 (1988).
[15]M. Frenklach and K.E. Spear, J. Mater. Res. **3**, 133 (1988).
[16]D.N. Belton and S.J. Harris, J. Chem. Phys. **96**, 2371 (1992).
[17]M. Frenklach, J. Chem. Phys. **97**, 5794 (1992).
[18]S.P. Mehandru and A.B. Andersson, J. Mater. Res. **5**, 2286 (1990).
[19]D.W. Brenner, Phys. Rev. B **42**, 9458 (1990).
[20]J.W. Mintmire *et al.*, in *Proceedings of the 2nd International Conference on the New Diamond Science and Technology*, edited by R. Messier and J. Glass, MRS Symposia Proceedings No. 162 (Materials Research Society, Pittsburgh, 1991).
[21]M.R. Pederson, K.A. Jackson, and W.E. Pickett, Phys. Rev. B **44**, 3891 (1991).
[22]T. Frauenheim and P. Blaudeck, Appl. Surf. Sci. **60-61**, 281 (1992).
[23]S.P. Mehandru and A.B. Andersson, Surf. Sci. **248**, 369 (1991).
[24]B.J. Garrison, E.J. Dawnkaski, D. Srivastava, and D.W. Brenner, Science **255**, 835 (1992).
[25]K. Larsson, S. Lunell, and J.O. Carlsson, Phys. Rev. B **48**, 2666 (1993).
[26]See, for example, K. Okada, S. Komatsu, T. Ishigaki, S. Matsumoto, and Y. Moriyoshi, J. Appl. Phys. **71**, 4920 (1992); B. Sun, X. Zhang, and Z. Lin, Phys. Rev. B **47**, 9816 (1993).
[27]M. Zhu, R.H. Hauge, J.L. Margrave, and M.P. D'Evelyn, in *Mechanisms for Step Growth on Diamond (100)*, MRS Symposia Proceedings No. 280 (Materials Research Society, Pittsburgh, 1993).
[28]T. Tsuno, T. Imai, Y. Nishibayashi, K. Hamada, and N. Fujimori, Jpn. J. Appl. Phys. **30**, 1063 (1991); H.G. Busmann, W. Zimmermann, H. Sprang, and H.J. Guntherodt, Diamond Relat. Mater. **1**, 979 (1992); L.F. Sutcu, C.J. Chu, M.S. Thompson, R.H. Hauge, J.L. Margrave, and M.P. D'Evelyn, J. Appl. Phys. **71**, 5930 (1992).
[29]Z.W. Hu, S.S. Jiang, P.Q. Huang, S.H. Li, Z.M. Zhang, C.Z. Ge, X.N. Zhao, and D. Feng, J. Phys. Condens. Matter **4**, 3753 (1992).
[30]D.R. Alfonso, S.E. Ulloa, and D.W. Brenner, Phys. Rev. B **49**, 4948 (1994).
[31]F.G. Celii and J.E. Butler, Annu. Rev. Phys. Chem. **42**, 643 (1991).
[32]M.N.R. Ashfold, P.W. May, and C.A. Rego, Chem. Soc. Rev. **23**, 21 (1994).
[33]O.F. Sankey and D.J. Niklewski, Phys. Rev. B **40**, 3979 (1989).
[34]O.F. Sankey, D.J. Niklewski, D.A. Drabold, and J.D. Dow, Phys. Rev. B **41**, 12 750 (1990).
[35]S.H. Yang, D.A. Drabold, and J.B. Adams, Phys. Rev. B **48**, 5261 (1993).
[36]D.A. Drabold, P.A Fedders, S. Klemm, and O.F. Sankey, Phys. Rev Lett. **67**, 2179 (1991); D.A. Drabold, R. Wang, S. Klemm, and O.F. Sankey, Phys. Rev. B **43**, 5132 (1991).
[37]J. Harris, Phys. Rev. B **31**, 1770 (1985).
[38]F. Herman and S. Skillman, *Atomic Structure Calculations* (Prentice-Hall, Englewood Cliffs, NJ, 1963).
[39]D.M. Ceperley and G.J. Alder, Phys. Rev. B **23**, 5048 (1981).
[40]J. Perdew and A. Zunger, Phys. Rev. B **23**, 5048 (1981).
[41]H.J. Monkhorst and J.D. Pack, Phys. Rev. B **13**, 5188 (1977).
[42]I.P. Batra, Phys. Rev. B **41**, 5048 (1990); D. J. Chadi, Phys. Rev. Lett. **43**, 43 (1987).
[43]J.Tersoff, Phys. Rev. B **37**, 6991 (1988).
[44]R.T. Morrison and R.N. Boyd, *Organic Chemistry*, 3rd ed. (Allyn and Bacon, Boston, 1973).
[45]D. Huang and M. Frenklach, J. Phys. Chem. **96**, 1868 (1992).
[46]X.Y. Zhu and J.M. White, Surf. Sci. **214**, 240 (1989).
[47]Using empirical potential expressions, we obtained no stable onefold bonding of C_2H_2 to the flat (111) surface.
[48]H.J.C. Berendsen, J.P.M. Postma, W.F. Gurentsen, A. Dinola, and J.R. Haak, J. Chem. Phys. **81**, 3684 (1984).
[49]Coordinates are available via alfonso@helios.phy.ohiou.edu.

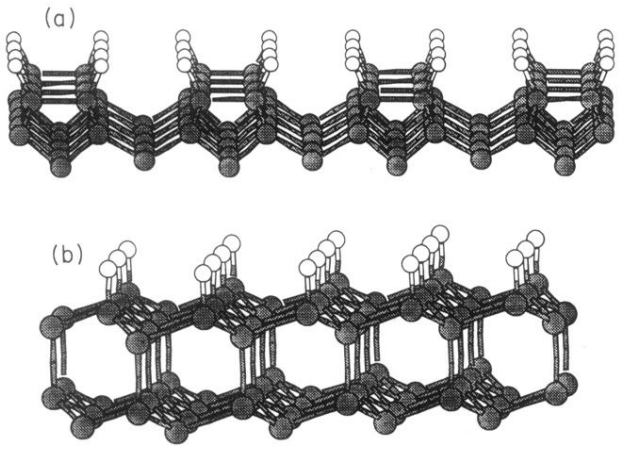

FIG. 1. Diagrams of (a) hydrogenated (100)-(2×1) and (b) hydrogenated (111) surfaces of diamond. Carbon atoms appear shaded.

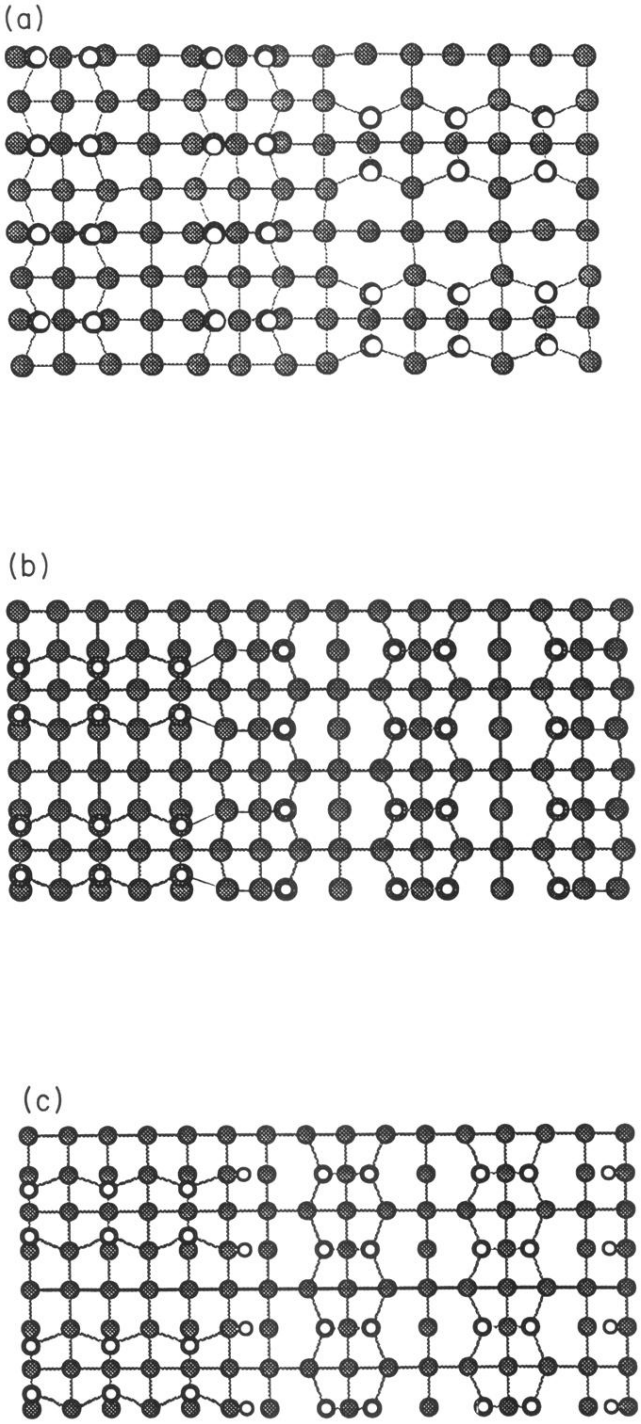

FIG. 2. The three types of diamond (100) stepped structures: (a) S_A, (b) $S_B(b)$, and (c) $S_B(n)$. Portions shown are the supercells for each step employed in this work (periodic 7×4 for the S_A structure and periodic 8×4 for the S_B structure). Carbon atoms appear shaded.

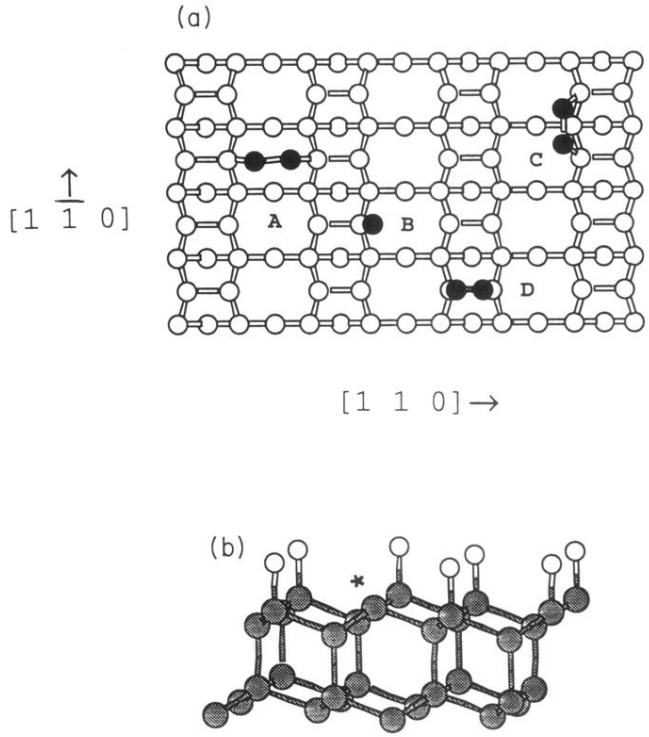

FIG. 3. (a) Top view of the diamond (100)-(2×1) surface showing various adsorption sites for the hydrocarbon adspecies. Shaded balls represent one- and two-carbon adspecies while white balls represent the substrate carbon atoms. *A* is a trough site along the [1 1 0] direction, *B* is a onefold binding site, *C* is a trough site in the [1 $\bar{1}$ 0] direction, and *D* is a bridge site. (b) Side view of a portion of a diamond (111) surface where the shaded balls represent the surface carbon. The marked atom is a radical surface carbon where the various hydrocarbon species are adsorbed.

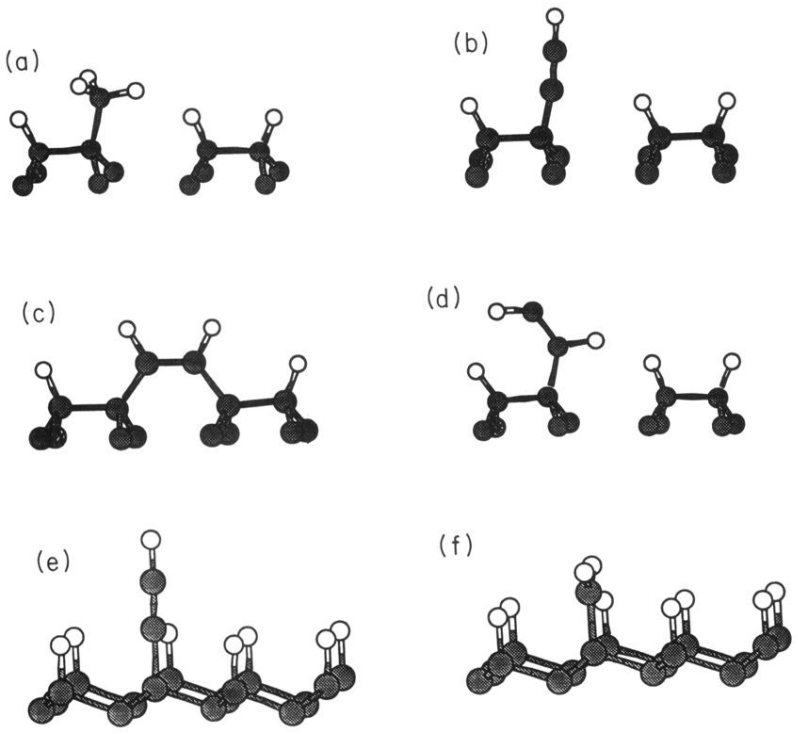

FIG. 4. Selected examples of configurations of the hydrocarbon admolecules on the flat diamond (100) and (111) surfaces. (a) CH_3 on (100), (b) C_2H on (100), (c) C_2H_2 on (100) (trough site along the [1 1 0] direction), (d) C_2H_2 on (100) (onefold), (e) C_2H on (111), and (f) CH_2 on (111).

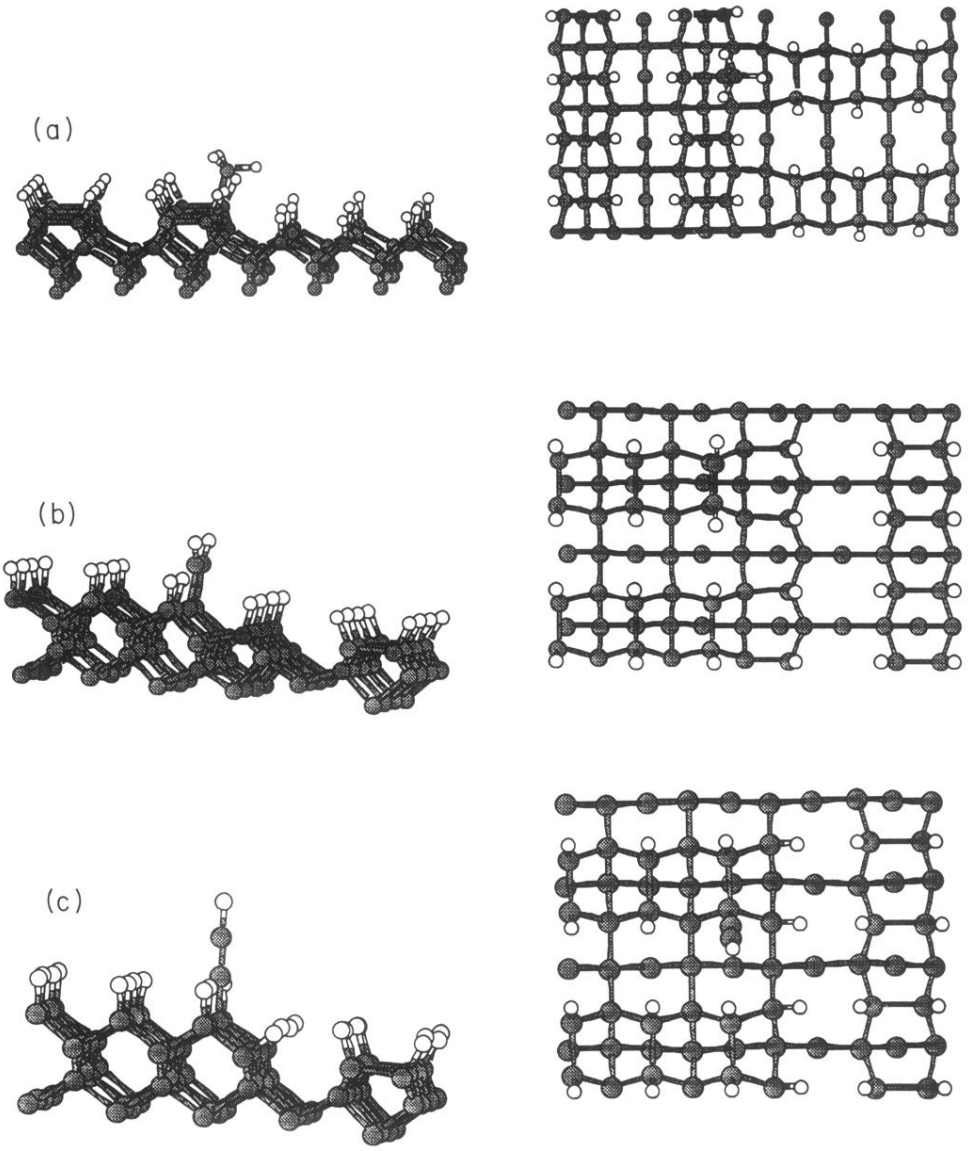

FIG. 5. Typical minimum-energy configurations for admolecule-stepped surface systems. Clusters shown are a portion of the unit cell employed in this work. (a) CH_3 on S_A, (b) C_2H_2 on $S_B(b)$ (bridge site), and (c) C_2H on $S_B(n)$. Carbon atoms appear shaded.